Journal of Sound and Vibration 473 (2020) 115246

Contents lists available at ScienceDirect

Journal of Sound and Vibration

journal homepage: www.elsevier.com/locate/jsvi

Modelling approach for MEMS transducers with rectangular clamped plate loaded by a thin fluid layer

K. Šimonová [a], P. Honzík [a,b,*], M. Bruneau [c], P. Gatignol [d]

[a] Czech Technical University in Prague, Faculty of Transportation Sciences, Konviktská 20, 110 00, Praha 1, Czech Republic
[b] Czech Technical University in Prague, Faculty of Electrical Engineering, Technická 2, 166 27, Praha 6, Czech Republic
[c] Laboratoire d'Acoustique de l'Université du Maine UMR CNRS 6613, Avenue Olivier Messiaen, Université du Maine, 72 017, Le Mans cedex 09, France
[d] Laboratoire Roberval UMR CNRS 7337, Université de Technologie de Compiègne, Département Génie Mécanique, Equipe Acoustique et Vibrations, Centre de Recherche de Royallieu, 60 203, Compiègne cedex, France

ARTICLE INFO

Article history:
Received 6 September 2019
Revised 2 February 2020
Accepted 10 February 2020
Available online 11 February 2020
Handling Editor: O. Guasch

Keywords:
Miniaturized transducer
MEMS microphone
Rectangular clamped plate
Plate-fluid coupling
Plate eigenfunctions

ABSTRACT

The paper is mainly concerned with the analytical approach of the behaviour of a two-dimensional miniaturized MEMS transducer, namely a rectangular or square clamped plate loaded by a fluid-gap (squeeze film), surrounded by a small cavity (reservoir), and excited by an incident acoustic field (assume to be uniform on the plate). Until now, the problem has not been analytically solved owing to the geometry of the device in conjunction with the nature of the diaphragm (elastic plate) and its boundary conditions (zero deflection and zero normal slope along all edges); namely analytical eigenfunctions do not exist for the clamped plate. On the other hand, the analytical approach classically used to express the acoustic field in the fluid-gap relies on a modal expansion which does not match correctly with both the displacement field of the diaphragm and the boundary conditions at the entrance of the reservoir. Then, two particular questions arise: how to derive analytically the modal behaviour of the loaded clamped plate, and what analytical approach for the acoustic field in the fluid gap is convenient to describe its coupling with the displacement field of the plate? The aim of the paper is both to provide basically an exact analytical approach and to handle a numerical implementation (FEM) against which the analytical results are tested.

1. Introduction

In the recent years, there has being growing interest in the design and the modelling of miniaturized (MEMS) electrostatic transducers [1,2] with a circular [3] or square [4,5] diaphragm (usually a membrane stretched on a rigid frame, a rectangular plate with different boundary conditions [6,7] or a planar microbeam [8,9]), loaded by a thin layer of thermo-viscous fluid [10,11] (of the same shape as the diaphragm) and a reservoir around it. The use of such transducers is rising not only in the domain of consumer audio devices, but also in the field of measurement applications such as antenna and noise monitoring using wireless sensor networks [12] where the increasing number of sensor nodes requires the development of low-cost sensors that provide sufficient measurement precision and reliability. Moreover, these kind of miniaturized devices, active (receivers or emitters) or passive devices, should be of interest for metrological applications under non-standard conditions, namely high frequency

* Corresponding author. Czech Technical University in Prague, Faculty of Transportation Sciences, Konviktská 20, 110 00, Praha 1, Czech Republic.
E-mail addresses: abramkar@fd.cvut.cz (K. Šimonová), honzikp@fd.cvut.cz (P. Honzík), michel.bruneau@univ-lemans.fr (M. Bruneau), philippe.gatignol@utc.fr (P. Gatignol).

https://doi.org/10.1016/j.jsv.2020.115246
0022-460X/

range (typically up to 500 kHz), gas mixtures, and various static pressures and temperatures [13], due to both their potentiality in terms of sensitivity (in particular) and their very small dimensions (surface area and thickness).

The characteristics of such miniaturized devices, manufactured using MEMS processes, may depart from the characteristics of the classical devices in three respects. First, the diaphragm could be no longer circular but square (this geometry sometimes presents serious analytical difficulties as we will see below), second the thickness of the significantly miniaturized diaphragm cannot be neglected against its other dimensions, thus it may no longer behave as a stretched membrane but, as a thin plate whose elasticity is characterised by its bending moment, and third such plate may be considered as clamped at its surrounding, that is to say the boundary conditions may involve not only a vanishing displacement but also a vanishing spatial derivative of it with respect to the in-plane normal to the boundary.

Therefore, to account for -i/the requirements mentioned above (non-standard conditions of use) which need deeper characterisation as the usual ones, -ii/the non-classical nature and geometry of the diaphragm in such devices (rectangular thin plate), and -iii/the edge conditions which relate to both the solution for the displacement field of the plate and its first spatial derivative (clamped plate), a dedicated analytic investigation that permits to describe the strong coupling between such a diaphragm (excited by an external acoustic field) and a thin fluid layer need to be addressed. Then, the aim of this paper is both to provide such analytical approach (sections 2 and 3) and to handle a numerical implementation (FEM) against which the analytical results are tested (section 4).

Classically, the analytical method used to calculate the behaviour of the diaphragm relies on the modal expansion for the displacement field (Dirichlet eigenmodes). But exact analytical eigenfunctions that would be solutions of the eigenvalue-problem associated to the clamped plate do not exist. To the best knowledge of the authors, the problem of the free or forced vibrations of thin clamped plates has not been fully solved yet without numerical integration, despite the wide range of approximate methods that have been employed to study this problem (see for example [15] chapter 4 and references at the end of this chapter and [16] chapters 7, 11, and 12). These methods or techniques include series methods, approximate analytical technique, finite difference techniques, Galerkin technique, Rayleigh-Ritz method, and more recently approximate analytical solutions [17,18], analytical expression based on the approximation of the FEM results [19]. All these approximate methods and other more or less derived from them prevent us from obtaining a tractable “exact” analytical approach to describe the strong coupling between the plate and the fluid gap loaded at its periphery by a reservoir. On the other hand, the analytical approach used to express the acoustic field in the fluid gap should not rely on a modal expansion, not only because it has marked shortcomings in terms of coupling with the modal expansion of the displacement field of the diaphragm, but also because it is not obvious how to match this expression with the boundary condition at the entrance of the reservoir, both especially when dealing with high frequency range.

The paper addresses two particular questions; namely, how to derive analytically the modal behaviour of the loaded clamped plate, and what analytical approach for the acoustic field in the fluid gap is convenient to describe its coupling with the displacement field of the plate? Such questions have a direct significance for the understanding of the phenomena which govern the behaviour of the transducer (displacement field of the plate and sensitivity of the electroacoustic transducer), especially under the non-standard conditions mentioned above. Moreover, as an extension to the responses to these questions, the approach presented here should not be limited to miniaturized devices: it is sufficiently broad to be of interest and the results may be helpful to those seeking benchmark solutions and analytic insight. Actually, other applications can be found in the field of vibroacoustics when a clamped plate is coupled to any acoustic field, such as membrane acoustic absorbers used in room acoustics [14].

After this Introduction, the second section of the paper details the utility of an auxiliary related problem (equation governing the movement of clamped elastic beams) to circumvent the difficulties that arise from the fact that there is no exact analytical eigenfunctions and eigenvalues to describe the modal behaviour of a rectangular clamped plate. The approach starts from the product of the orthonormal eigenfunctions for elastic beams in both the in-plane (x - and y -) directions, which satisfy the boundary conditions of the clamped plate; it makes possible a modal expansion which is a solution of the non-homogeneous equation governing the displacement field of the plate, leading to a quite simple analysis of the behaviour of the clamped plate via an elastic coupling, in addition to the existing coupling between the plate and the acoustic field in the thin fluid layer. The relevant point here is that, with such construction of the solution (truncated modal expansion), the satisfaction of the boundary conditions follows automatically from the fact that each of the eigenfunctions satisfies these boundary conditions. The eigenfunctions and eigenvalues of the plate are discussed in the Appendix A.

In the third section, the analytical solution for the acoustic field in the fluid-gap is presented. It does not make use of modal expansion but of an integral formulation with an appropriate two-dimensional Green’s function (not expressed as sum over eigenfunctions), which allows avoiding the procedural difficulties mentioned above [5]. This solution is also assumed to have the same symmetry as the plate, which makes possible to express the problem for the acoustic pressure in the first quadrant only. The wavenumber associated to this acoustic field accounts for both the vortical movement due to the shear viscosity effects and the entropic movement due to thermal conduction effects (this last effect is not negligible because the compressibility of the gas is a complex function, tending to the real isothermal one in the lower frequency range and to the real adiabatic one in the higher frequency range). The acoustic field in the small reservoir is assumed to be uniform. At the end of the section, we are left with two coupled equations which relate respectively the acoustic pressure inside the fluid behind the plate to the displacement field of the plate and, conversely, equation which relates the displacement field of the plate to the acoustic pressure behind the plate. Then the coefficients of the expansion of the displacement field of the plate are given by the solutions of a set of linear algebraic equations. Note that the flow inside the fluid layer can be considered or not as continuous fluid flow depending on the values of the Knudsen number defined as the ratio of the molecular mean free path (at the static pressure considered) to the

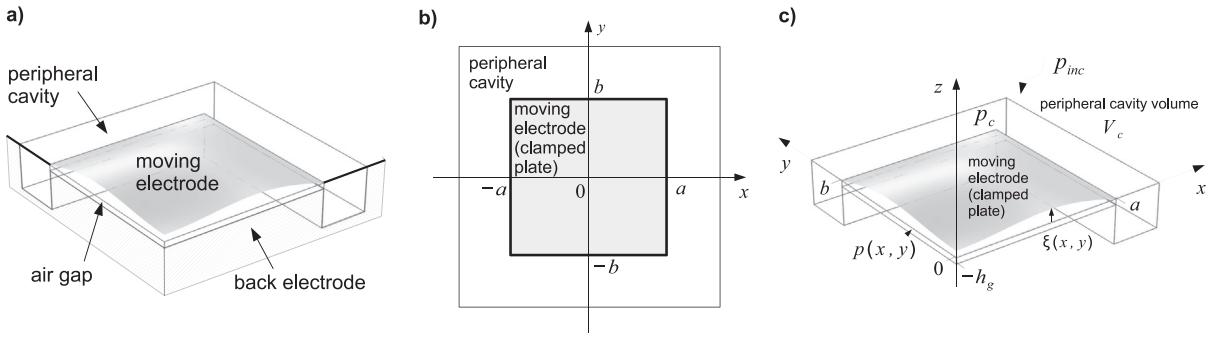

Fig. 1. Geometry of the system: a) cut of one quarter of the device, b) top view of the device, the dimensions of the square plate and c) geometry of the transducer and corresponding notation in the first quadrant.

characteristic length of the acoustic flow, namely here the thickness of the fluid layer [20]: in the frequency range considered herein (up to 1 MHz) and for the order of magnitude of the thickness of the fluid gap (around 10 μm or larger), the continuous flow regime can be assumed because the mean free path remains much lower than this thickness (except for very low static pressure, i.e. less than 10^2 Pa for the air).

2. The device, statement of the problem

The transducer consists of a rectangular (or square) elastic clamped plate (moving electrode) set at the coordinate $z = 0$ and fixed at its periphery to a rigid frame where the coordinates x and y are equal to $\pm a$ and $\pm b$ respectively (with a and $b > 0$). A thin fluid layer (more often an air gap) of thickness h_g is trapped between the plate and a back rigid electrode having the same shape as the elastic plate. This fluid layer is loaded at its periphery by a small cavity (surrounding reservoir) (see Fig. 1).

A monochromatic incident acoustic wave of angular frequency ω impinges the plate; the pressure field of complex amplitude on the plate denoted below p_{inc}, is assumed to be uniform over the entire surface of the plate. Then, symmetrical movement with respect to the axes passing through the centre of the plate and parallel to its edges is the only one considered herein (in addition, the sensitivity depends only on this movement). Note that the time dependence $e^{i\omega t}$ has been suppressed throughout the entire analysis below.

2.1. The displacement field of the rectangular clamped plate

The normal displacement field of the loaded plate is positively evaluated along the z-axis. The set of equations which govern its complex amplitude can be written classically as [15]:

$$\left[\frac{\partial^4}{\partial x^4} + 2\frac{\partial^4}{\partial x^2 \partial y^2} + \frac{\partial^4}{\partial y^4} - k_p^4\right] \xi(x,y) = \frac{1}{D}\left[-p_{inc} + p\,(x,y)\right],\ x \in (-a,a), y \in (-b,b), \tag{1}$$

$$\xi\,(x,y) = \frac{\partial}{\partial x}\xi\,(x,y) = 0, x = \pm a, \forall y \in (-b,b)\,, \tag{2}$$

$$\xi\,(x,y) = \frac{\partial}{\partial y}\xi\,(x,y) = 0, y = \pm b, \forall x \in (-a,a)\,, \tag{3}$$

where $D = \frac{Eh_p^3}{12(1-\nu^2)}$ is the flexural rigidity, ν being the Poisson's ratio, E the Young's modulus, h_p is the thickness of the plate, $k_p^4 = \frac{M_s}{D}\omega^2, M_s = h_p\rho_p$ is the mass per unit area, ρ_p being the density of the plate.

As mentioned in the introduction, there is no exact analytical eigenfunction to describe the modal behaviour of the rectangular (or square) clamped plate and then no method to solve directly the problem with any "source" term that depends on the coordinates x and y [in the right side of equation (1)]. That is the reason why the construction of the solutions of equations (1)–(3) presented below relies on the known modal wave functions of the 1-D beam (normalized eigenfunctions ϕ_m) that are solutions of the homogeneous equations

$$\left[\frac{\mathrm{d}^4}{\mathrm{d}x^4} - \alpha_m^4\right]\phi_m\,(x) = 0 \quad \text{and} \quad \left[\frac{\mathrm{d}^4}{\mathrm{d}y^4} - \beta_m^4\right]\phi_m\,(y) = 0, \tag{4}$$

and subject to the boundary conditions of the clamped plate, i.e.

$$\phi_m\,(-u) = \phi_m\,(u) = \phi'_m\,(u) = \phi'_m\,(-u) = 0, \tag{5}$$

with $u = a$ or b, and where $'$ means spatial derivative; these solutions for the coordinate x (the results for the coordinate y are similar), eigenfunctions and eigenvalues, take the following form, symmetric and antisymmetric form respectively:

$$\phi_m^s(x) = \frac{1}{\sqrt{2a}}\left[\frac{\cos(\alpha_m^s x)}{\cos(\alpha_m^s a)} - \frac{\cosh(\alpha_m^s x)}{\cosh(\alpha_m^s a)}\right], \quad \text{with} \quad \tan\left(\alpha_m^s a\right) = -\tanh\left(\alpha_m^s a\right), \tag{6}$$

$$\phi_m^a(x) = \frac{1}{\sqrt{2a}}\left[\frac{\sin(\alpha_m^a x)}{\sin(\alpha_m^a a)} - \frac{\sinh(\alpha_m^a x)}{\sinh(\alpha_m^a a)}\right], \quad \text{with} \quad \tan\left(\alpha_m^a a\right) = \tanh\left(\alpha_m^a a\right), \tag{7}$$

the symmetrical solution being the only one useful in our problem, as mentioned above (henceforth, ϕ_m and α_m will denote the symmetrical versions ϕ_m^s and α_m^s (6) respectively).

We assume that the displacement field of the plate satisfying the governing equations (1)–(3) may be predicted in the form, with some truncation condition,

$$\xi(x,y) = \sum_{mn}^{\infty} \xi_{mn}\psi_{mn}(x,y), \tag{8}$$

$$\text{where} \quad \psi_{mn}(x,y) = \phi_m(x)\,\phi_n(y), \tag{9}$$

even though $\psi_{mn}(x,y)$ does not satisfy the eigen-problem of the plate but satisfy only the boundary conditions (2) and (3), the coefficients ξ_{mn} reflecting here an elastic coupling mechanism between the 1-D modal solutions along the two axes x and y. On substituting expression (8) into equation (1) it is found that

$$\sum_{m,n}\xi_{mn}\left(\alpha_m^4 + \beta_n^4 - k_p^4\right)\psi_{mn}(x,y) + 2\sum_{m,n}\xi_{mn}\,\phi_m''(x)\,\phi_n''(y) = \frac{1}{D}\left[-p_{inc} + p(x,y)\right], \tag{10}$$

where $(''$) means second spatial derivative.

Accounting for the orthogonality of the normalized modal functions $\psi_{mn}(x,y)$, the inner product defined as $\left[\int_{-a}^{a}\int_{-b}^{b} f_1(x,y) f_2(x,y)\,\mathrm{d}x\mathrm{d}y\right]$ of equation (10) and $\psi_{m'n'}(x,y)$ leads readily to

$$\left(K_{m'n'}^4 - k_p^4\right)\xi_{m'n'} + 2\sum_{mn}\sigma_{mm'}\tau_{nn'}\xi_{mn} = Q_{m'n'}, \tag{11}$$

where

$$\sigma_{mm'} = \int_{-a}^{a}\phi_m''(x)\,\phi_{m'}(x)\,\mathrm{d}x \qquad \text{and} \qquad \tau_{nn'} = \int_{-b}^{b}\phi_n''(y)\,\phi_{n'}(y)\,\mathrm{d}y, \tag{12}$$

$$Q_{m'n'} = \int_{-a}^{a}\int_{-b}^{b}\frac{1}{D}\left[-p_{inc} + p(x,y)\right]\psi_{m'n'}(x,y)\,\mathrm{d}x\mathrm{d}y, \tag{13}$$

$$K_{mn}^4 = \alpha_m^4 + \beta_n^4, \tag{14}$$

α_m and β_n being related together by $\alpha_m/\beta_n = b/a$. It is worth noting that the matrices $\sigma_{mm'}$ and $\tau_{nn'}$ are equal, to within a factor, and that they are symmetrical as a result of equations (5) and (12).

The elastic coupling mentioned above is represented by the second term in the left hand side of equation (11). But another coupling will occur: the one due to the acoustic pressure field behind the plate $p(x,y)$ because it depends on the displacement field $\xi(x,y)$ (see next section). Note that solving the set of equation (11) with $Q_{m'n'} = 0$ leads to expressions of eigenfunctions and eigenvalues of the problem (see Appendix A).

3. The acoustic field inside the air gap, coupling with the plate displacement

In what follows, in order to simplify the presentation, the device is assumed to be square ($a = b$) without loss of generality (this corresponds to the systems manufactured in practice) and the acoustic field in the fluid enclosed behind the plate is assumed to have the same symmetry as the plate. Owing to this symmetry, it is appropriate to express the solutions only in the first quadrant, assuming that these solutions can be considered either over any quadrant or over the whole plate (changing the sign of a when the coordinates are negative).

The thickness of the air-gap h_g is smaller than - or of the same order of magnitude as - the thickness of the viscous and the thermal boundary layers, the pressure variation is assumed to be uniform through that (very small) thickness, and the acoustic pressure field is assumed to be uniform inside the peripheral cavity (volume V_c) because its dimensions are smaller than half wavelength in the frequency range considered.

The properties of the fluid (air) are given by the ρ_0, the adiabatic speed of sound c_0, the heat capacity at constant pressure per unit mass C_p, the specific heat ratio γ, the shear viscosity coefficient μ, and the thermal conduction coefficient λ_h. The wavenumber associated to the acoustic field in the air-gap, which account for both the vortical movement due to viscosity

effects and the entropic movement due to thermal conduction effects inside the thermo-viscous boundary layers, take the following form [5]:

$$\chi^2 = \frac{\omega^2}{c_0^2}\frac{1+(\gamma-1)\left(1-F_h\right)}{F_v} \tag{15}$$

where

$$\begin{aligned} F_v &= 1-\tan\left(k_v h_g/2\right)/\left(k_v h_g/2\right), \\ F_h &= 1-\tan\left(k_h h_g/2\right)/\left(k_h h_g/2\right), \end{aligned} \tag{16}$$

$$\text{with}\quad k_v = \left[(1-\mathrm{i})/\sqrt{2}\right]\sqrt{\rho_0\omega/\mu}\quad\text{and}\quad k_h = \left[(1-\mathrm{i})/\sqrt{2}\right]\sqrt{\rho_0\omega C_p/\lambda_h}. \tag{17}$$

Assuming that the plate behaves as an extended source described by the z - component of its volume velocity per unit volume positive when directed along the z - axis, denoted $\zeta\xi(x,y)$, the propagation equation take the following form:

$$\left[\frac{\partial^2}{\partial x^2}+\frac{\partial^2}{\partial y^2}-\chi^2\right]p(x,y) = -\zeta\xi(x,y) \tag{18}$$

$$\text{where}\quad \zeta = \rho_0\omega^2/\left(h_g F_v\right). \tag{19}$$

Furthermore, the total velocity flow rate $-\left[F_v/\left(\mathrm{i}\omega\rho_0\right)\right]2ah_g\partial_{\overline{n}}p$ that enter the reservoir in any boundary $x,y=\pm a$, equal to the ratio p_c/Z_c, where $Z_c=\rho_0 c_0^2/\left(\mathrm{i}\omega V_c\right)$ is the input impedance of the reservoir, leads to

$$\partial_{\overline{n}}p = \Lambda_c p_c\quad\text{with}\quad \Lambda_c = \left(-\mathrm{i}\omega\rho_0\right)/\left(2ah_g F_v Z_c\right), \tag{20}$$

where the normal derivative $\partial_{\overline{n}}p$ denotes the mean values along the y - axis and x - axis of the derivatives $\partial_x p(a,y)$ and $\partial_y p(x,a)$ respectively.

In so far as the chosen Green's function satisfies, at $x=0$ and $y=0$, the same Neumann's boundary condition as the pressure variation (symmetrical movement), i.e. the first derivative normal to these boundaries of each quadrant vanishes, the integral equation for the pressure variation in the fluid gap $x,y\in(0,a)$ takes the following form [5], accounting for equation (20):

$$p(x,y) = \int_0^a\int_0^a G\left(x,x_0;y,y_0\right)\zeta\xi\left(x_0,y_0\right)\mathrm{d}x_0\mathrm{d}y_0 + p_c I_G(x,y) \tag{21}$$

$$I_G(x,y) = \int_0^a\left[\Lambda_c G(x,x_0;y,a)-\partial_{y_0}G(x,x_0;y,a)\right]\mathrm{d}x_0 + \int_0^a\left[\Lambda_c G(x,a;y,y_0)-\partial_{x_0}G(x,a;y,y_0)\right]\mathrm{d}y_0 \tag{22}$$

where, on the boundaries in equation (22), the functions $p\left(x_0,a\right)$ and $p\left(a,y_0\right)$ have been replaced by their mean values p_c respectively along the x - axis and y - axis, and where the Green function can be taken as

$$G(x,x_0;y,y_0) = g(x,x_0;y,y_0)+g(x,-x_0;y,y_0)+g(x,x_0;y,-y_0)+g(x,-x_0;y,-y_0), \tag{23}$$

$$\text{with}\quad g(x,x_0;y,y_0) = -\mathrm{i}H_0^-\left(\chi\sqrt{\left(x-x_0\right)^2+\left(y-y_0\right)^2}\right)/4, \tag{24}$$

H_0^- denoting the Hankel function of the second kind of order "0".

It remains to express the pressure variation $p(x,y)$ (equation (21)) as a function of the displacement field $\xi(x,y)$ only, namely to express the pressure variation inside the reservoir p_c as a function of $\xi(x,y)$. This last expression is given approximately by the mean value of the pressure $p(x,y)$ over the length of any external edge of the quadrant, namely, owing to the symmetry, $p_c=\langle p\rangle=(1/a)\int_0^a p(x,a)\,\mathrm{d}x$ or equivalently $p_c=\langle p\rangle=(1/a)\int_0^a p(a,y)\,\mathrm{d}y$

$$p_c \cong \frac{1}{1+\langle I_G(x,a)\rangle}\int_0^a\int_0^a\langle G(x,x_0;a,y_0)\rangle\,\zeta\xi\left(x_0,y_0\right)\mathrm{d}x_0\mathrm{d}y_0. \tag{25}$$

Therefore, the sought-after solution (21) can be expressed as

$$p(x,y) = \zeta\int_0^a\int_0^a\left[G(x,x_0;y,y_0)+\frac{I_G(x,y)\langle G(x,x_0;y,y_0)\rangle}{1+\langle I_G(x,a)\rangle}\right]\xi(x_0,y_0)\mathrm{d}x_0\mathrm{d}y_0. \tag{26}$$

Utilizing (8) and (26) it follows readily that

$$p(x,y) = \sum_{m,n}B_{mn}(x,y)\,\xi_{mn} \tag{27}$$

Table 1
Properties of the air.

Parameter	Value	Unit
Adiabatic sound speed c_0	343.2	m s^{-1}
Air density ρ_0	1.2	kg m^{-3}
Shear dynamic viscosity μ	$1.814 \cdot 10^{-5}$	Pa s
Thermal conductivity λ_h	$25.77 \cdot 10^{-3}$	W m^{-1} K^{-1}
Specific heat coefficient at constant pressure per unit of mass C_p	1005	J kg^{-1} K^{-1}
Ratio of specific heats γ	1.4	–

where the known functions $B_{mn}(x,y)$ are given by

$$B_{mn}(x,y) \cong \zeta \int_0^a \int_0^a \left[G(x,x_0;y,y_0) + \frac{I_G(x,y)\,\langle G(x,x_0;y,y_0)\rangle}{1+\langle I_G(x,a)\rangle} \right] \psi_{mn}(x_0,y_0)\mathrm{d}x_0\mathrm{d}y_0. \tag{28}$$

It follows readily from the couple of equations (11) and (27) that the unknown coefficients ξ_{mn}, which lead to the displacement field of the plate $\xi(x,y)$, are solution of the following set of linear algebraic equations

$$H_{m'n'}\xi_{m'n'} + \sum_{mn} C_{mn,m'n'}\xi_{mn} = -E_{m'n'} + \sum_{mn} A_{mn,m'n'}\xi_{mn} \tag{29}$$

or in the matrix form

$$([\mathbb{A}] - [\mathbb{C}] - [\mathbb{H}])(\Xi) = (E), \tag{30}$$

where $[\mathbb{A}]$ is the "plate-fluid" coupling square matrix of elements

$$A_{mn,m'n'} = \int_{-a}^{a} \int_{-a}^{a} B_{mn}(x,y)\,\psi_{m'n'}(x,y)\,\mathrm{d}x\mathrm{d}y, \tag{31}$$

$[\mathbb{C}]$ the "internal elastic plate" coupling square matrix of elements

$$C_{mn,m'n'} = 2\,D\,\sigma_{mm'}\sigma_{nn'}, \tag{32}$$

$[\mathbb{H}]$ the diagonal matrix of elements (which include the effects of the eigenvalues)

$$H_{m'n'} = D\left[K^4_{m'n'} - k_p^4\right], \tag{33}$$

and where$[\Xi]$ and $[\mathbb{E}]$ are the column matrices of respectively the unknown coefficients $\xi_{m'n'}$ and the elements $E_{m'n'}$, which involve the external source pressure field p_{inc},

$$E_{m'n'} = p_{inc} \int_{-a}^{a} \int_{-a}^{a} \psi_{m'n'}(x,y)\,\mathrm{d}x\mathrm{d}y. \tag{34}$$

4. Analytical results and comparison with numerical (FEM) ones

In this section the analytical results (displacement field of the square plate, sensitivity of the receiving transducer) obtained from the above described procedure are compared with the reference numerical solutions provided by the software Comsol Multiphysics, version 5.4. In the latter, the formulation for the acoustic field in thermoviscous fluid, involving the particle velocity $\vec{v}$, the temperature variation τ and the acoustic pressure p, implemented in the Acoustics Module of Comsol [21] has been coupled with the classical linear shell formulation employed by the Structural Mechanics Module [22]. The use of such formulations in the modelling of electroacoustic transducers is described for example in Ref. [20]. The mesh consisted of tetrahedral elements combined with layered prism elements (in the boundary layers) and the number of degrees of freedom was 457 157. More details on the time of calculation are given at the end of this section. The properties of the air and the dimensions of the system along with the material properties of the plate used herein are given in Tables 1 and 2 respectively.

The real parts of the displacement $\xi(x,y)$ of the square clamped plate (used as a moving electrode of the receiving transducer presented herein) at four different frequencies are depicted in Fig. 2. The upper row of the figure shows the results of the above described method calculated using the nine first terms in the series (8) $(m,n = 1,2,3)$ for the incident acoustic pressure $p_{inc} = 1$ Pa. The reference numerically calculated results for the plate displacement are presented in the lower row of the figure using the same range of values and colormaps as for the upper row. Very good agreement between the analytical and numerical results can be found, especially at 10 kHz and 200 kHz. At 520 kHz the amplitude is slightly overestimated by the analytical method, at 800 kHz the quasi-circular shape of the analytically calculated displacement does not represent exactly the small peaks in the reference numerical result. These discrepancies (caused probably by the approximations in the analytical solution) remain very small and seem to have negligible impact on the mean displacement of the plate (the variable of interest when searching for the acoustic pressure sensitivity of the receiving transducer, see below).

Table 2
Dimensions of the system and material properties of the plate.

Parameter	Value	Unit
Plate half side a	$0.5 \cdot 10^{-3}$	m
Plate thickness h_p	10^{-6}	m
Peripheral cavity volume V_c	10^{-10}	m^3
Air-gap thickness h_g	10^{-6}	m
Plate density ρ_p	2329	kg m^{-3}
Young's modulus E	160	G Pa
Poisson's ratio ν	0.27	–

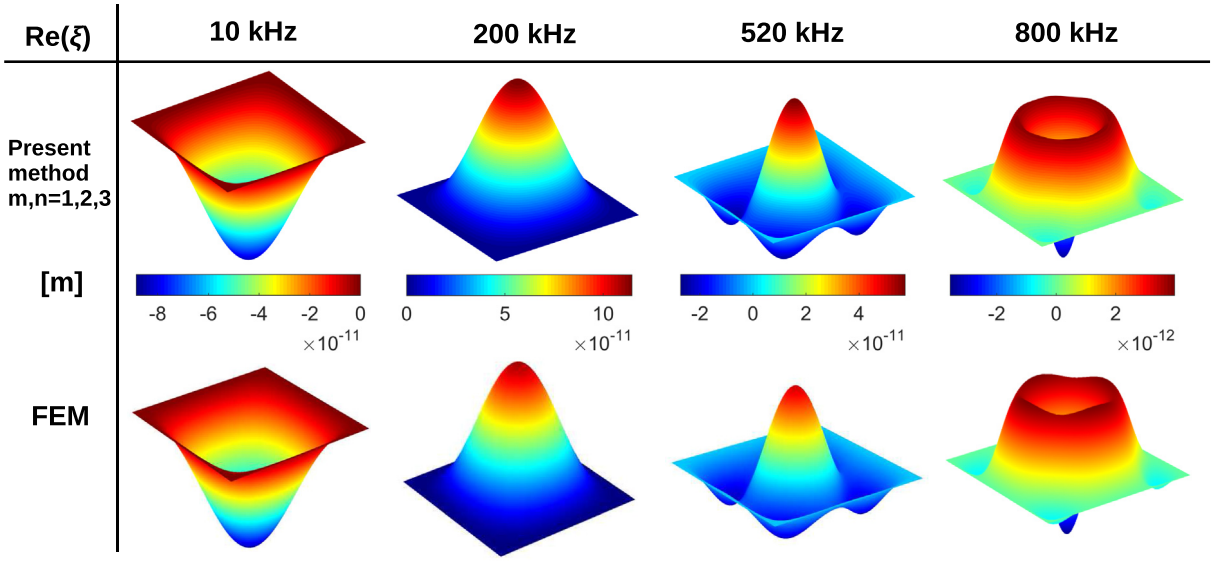

Fig. 2. Real part of the displacement field of the square plate $\xi(x, y)$ at 10 kHz, 200 kHz, 520 kHz and 800 kHz: comparison between the results of the present method (upper figures) and the reference FEM solutions (lower figures).

The acoustic pressure sensitivity of the electrostatic receiving transducer $\sigma = -U_0\overline{\xi}/(h_g p_{inc})$, where $\overline{\xi} = [\iint_{S_e} \xi(x,y) dS_e]/S_e$ is the mean displacement of the plate over the surface of the backing electrode $S_e = 4a^2$ and U_0 is the polarization voltage, is presented in Fig. 3 for different number of terms in the series (8). Fig. 3a) shows a very good agreement between the analytical and reference numerical results in a large frequency range (from 10 Hz up to approximately 1 MHz) except for the case of $m, n = 1$ (only one term in the series) at the frequencies above the first resonance frequency. The detail of the sensitivity in the passband of the transducer (10 Hz - 100 kHz) presented in Fig. 3b) shows that the difference between the analytical and the numerical results decreases with the increasing number of terms in the series (8). Note that this difference does not exceed 0.25 dB in the audio frequency range (20 Hz - 20 kHz) when the first nine terms in the series ($m, n = 1, 2, 3$) are used (and does not exceed 0.3 dB for $m, n = 1, 2$ and 0.75 dB for $m, n = 1$), which is very low comparing for example to Ref. [18] where this difference is around 3 dB. Fig. 3c) and d) show respectively the details of the sensitivity near the first resonance (50 kHz–220 kHz) and in the higher frequency range (300 kHz - 1.3 MHz) where the solution with four terms in the series (8) ($m, n = 1, 2$) is no more able to provide correct results above approximately 1 MHz while the solution with nine terms ($m, n = 1, 2, 3$) still remains very close to the reference numerical one.

Concerning the time of calculation, the reference numerical solution with the above given parameters took, on average, 134 s per one frequency point on a computer with two eight-core Intel Xeon processors running at 2.4 GHz while 28 GB of RAM has been used. The time of the analytical calculations, herein implemented in Matlab software, depends on many parameters. For example the calculation at lower frequencies took usually less time. The precision of the numerical integration influences the time of calculation of each member of the matrix $\mathbb{A}$ in equation (30) (adaptative Simpson quadrature has been used here, the precision being given by the difference between the results of the last two iterations, called tolerance). The most important parameter is the number of the terms of the series (8) which determines the size of matrices in equation (30). Since Comsol Multiphysics employs parallel computation on all the sixteen cores, the fair comparison between the calculation time necessary for the analytical result and for the numerical one requires the parallel computation in Matlab, achieved here by calculating more frequencies at the same time (using the *parfor* loop). The average time per one frequency point calculated as the total time divided by the number of frequency points was 1.22 s for $m, n = 1$, 12.23 s for $m, n = 1, 2$ and 63.79 s for $m, n = 1, 2, 3$, for the results presented in Fig. 3, a high precision of the numerical integration (tolerance of 10^{-6}) being used. This shows that the

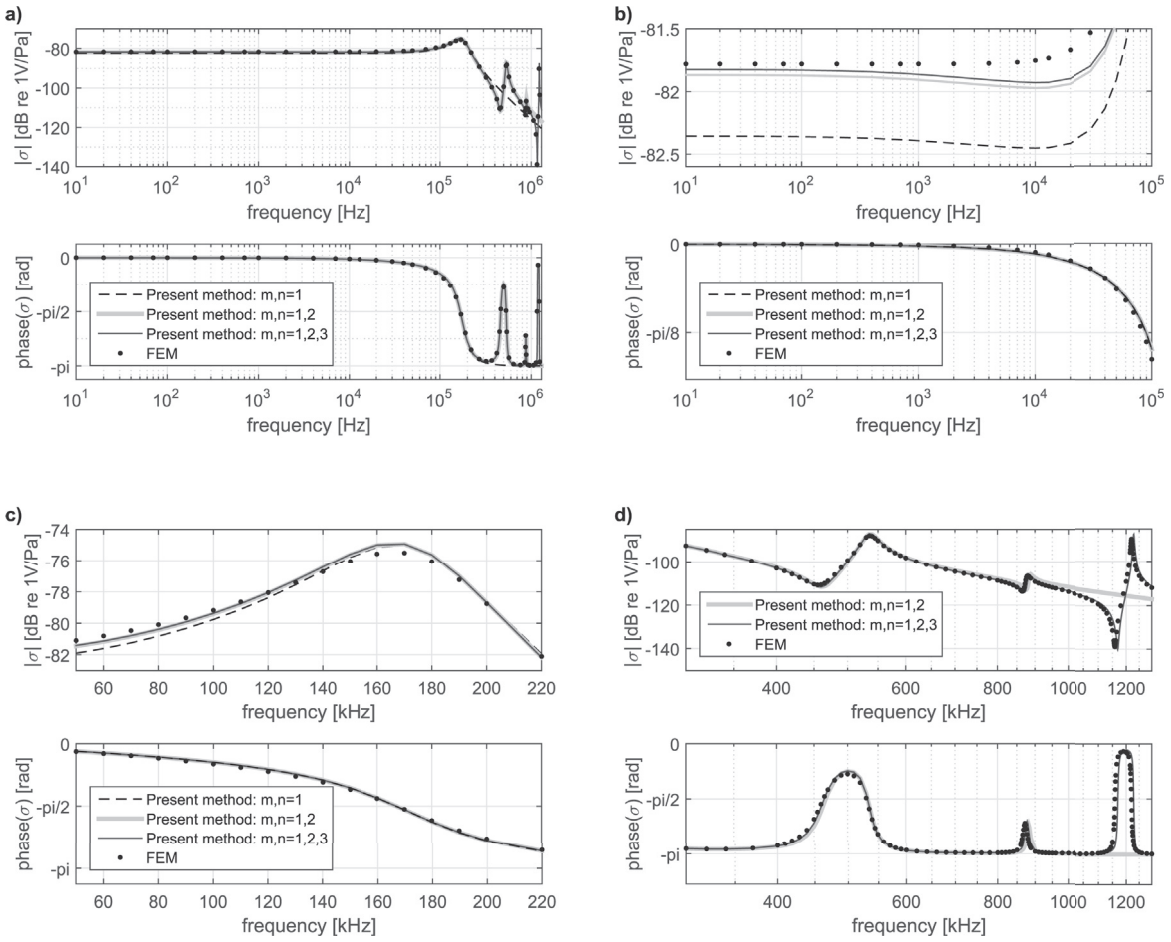

Fig. 3. Magnitude (upper curves) and phase (lower curves) of pressure sensitivity of the transducer: comparison of the analytical result using only the first mode $m, n = 1$ (dashed line), the first four modes $m, n = 1, 2$ (thick grey line) and the first nine modes $m, n = 1, 2, 3$ (thin black line) with the numerical result (black points); a) in the whole frequency range of interest (10 Hz - 1.3 MHz), b) in the lower frequency range (10 Hz - 100 kHz), c) near the first resonance (50 kHz–220 kHz), and d) in the higher frequency range (300 kHz - 1.3 MHz).

use of four terms ($m, n = 1, 2$) of the series (8) is a good compromise for the receiving transducers while the use of nine terms ($m, n = 1, 2, 3$) takes much more time and brings only small amount of precision in the passband of the transducer (see Fig. 3b). It is worth noting that the implementation in Matlab was not optimized for speed, the use of other languages, such as C, could lead to much faster computation.

5. Conclusions

The analytical approach of the behaviour of a two-dimensional miniaturized transducer containing a rectangular or square clamped plate loaded by a fluid gap surrounded by a small peripheral cavity has been developed. The displacement field of the plate has been searched for in the form of series expansion over the functions expressed as a product of the orthonormal eigenfunctions of elastic beams (clamped at both ends) in both the in-plane (x and y) directions. These functions satisfy the boundary conditions of the clamped plate and although they do not satisfy the eigen-problem of the plate, the coefficients of the series include the effects of an internal elastic coupling between the two 1D solutions, which makes the series expansion solution of the plate equation. In order to express the acoustic pressure field in the air gap, an integral formulation with an appropriate Green's function (not expressed as a sum over eigenfunctions), which accounts for the effect of thermoviscous losses through the complex wavenumber, has been used. The coupling of the plate displacement and the loading acoustic pressure field leads to the simple set of linear algebraic equations expressed herein in the matrix form.

Very good agreement between the analytical results obtained using the method described herein and the reference numerical (FEM) solution can be observed for both the displacement field of the plate and the acoustic pressure sensitivity of the receiving transducer. The method described herein thus provides analytical results whose precision is comparable with the numerically

calculated results (in the frequency range of interest) with much lower computational costs. Finally, note that this approach can be useful not only in the domain of miniaturized transducers but in much larger variety of devices.

CRediT authorship contribution statement

K. Šimonová: Conceptualization, Methodology, Data curation, Formal analysis, Writing - original draft. **P. Honzík:** Conceptualization, Methodology, Data curation, Formal analysis, Writing - original draft. **M. Bruneau:** Conceptualization, Methodology, Formal analysis, Writing - original draft, Writing - review & editing. **P. Gatignol:** Conceptualization, Methodology, Formal analysis, Writing - original draft, Writing - review & editing.

Acknowledgement

This work was supported by the Grant Agency of the Czech Technical University in Prague, grant No. SGS18/200/OHK2/3T/16. The authors would like to acknowledge the "HUB Acoustique" program within the "Le Mans Acoustique" (LMAc) project.

Appendix A. Approximated eigenfunctions of the clamped rectangular plate

We use below the following notation: $[\mathbb{C}]$ is the "internal elastic plate coupling" square matrix of elements

$$C_{mn,m'n'} = 2\,\sigma_{mm'}\tau_{nn'}, \tag{A.1}$$

$[\mathbb{H}]$ the diagonal matrix of elements (which include the effects of the eigenvalues k_i)

$$H_{m'n'} = K^4_{m'n'} - k_i^4, \tag{A.2a}$$

$$[\mathbb{U}] = K^4_{m'n'}\,[\mathbb{I}]\,, \tag{A.2b}$$

and (Ξ) is the column matrix of the unknown coefficients ξ_{mn}. Note that the elements of the matrix $[\mathbb{C}]$ can be written as $C_{mn,m'n'} = C_{N,N'}$ from a conventional choice of the couples (m,n) and that this matrix $C_{N,N'}$ is symmetrical like the matrices of elements $\sigma_{mm'}$ and $\tau_{nn'}$. As a result, the matrix $[\mathbb{C}] + [\mathbb{U}]$ is symmetrical and the eigenvalues k_i^4 are real.

Solving the set of linear equation (11) with $Q_{mn} = 0$, namely

$$([\mathbb{C}] + [\mathbb{H}])\,(\Xi) = (0), \quad \text{or} \tag{A.3a}$$

$$\left([\mathbb{C}] + [\mathbb{U}] - k_i^4\,[\mathbb{I}]\right)(\Xi) = (0), \tag{A.3b}$$

for any value of the indices [equation (A.3a) being valid for all modes denoted with the indices "i"], leads to the eigenvalues k_i of the unloaded clamped plate modes, solutions of the following equation

$$\det\left([\mathbb{C}] + [\mathbb{U}] - k_i^4\,[\mathbb{I}]\right) = 0, \tag{A.4}$$

and the corresponding expressions of the orthogonal eigenfunctions denoted below $\psi_i(x,y)$

$$\psi_i(x,y) = \sum_{mn}^{\infty} \xi_{i,mn}\psi_{mn}\,(x,y)\,. \tag{A.5}$$

Note that the orthogonality and completeness of the modal functions $\psi_{mn}\,(x,y)$ can be readily derived using the procedure similar to the one given in Appendix C of [20]. An extension of this method can be used to demonstrate the orthogonality of the eigenfunction $\psi_i\,(x,y)$.

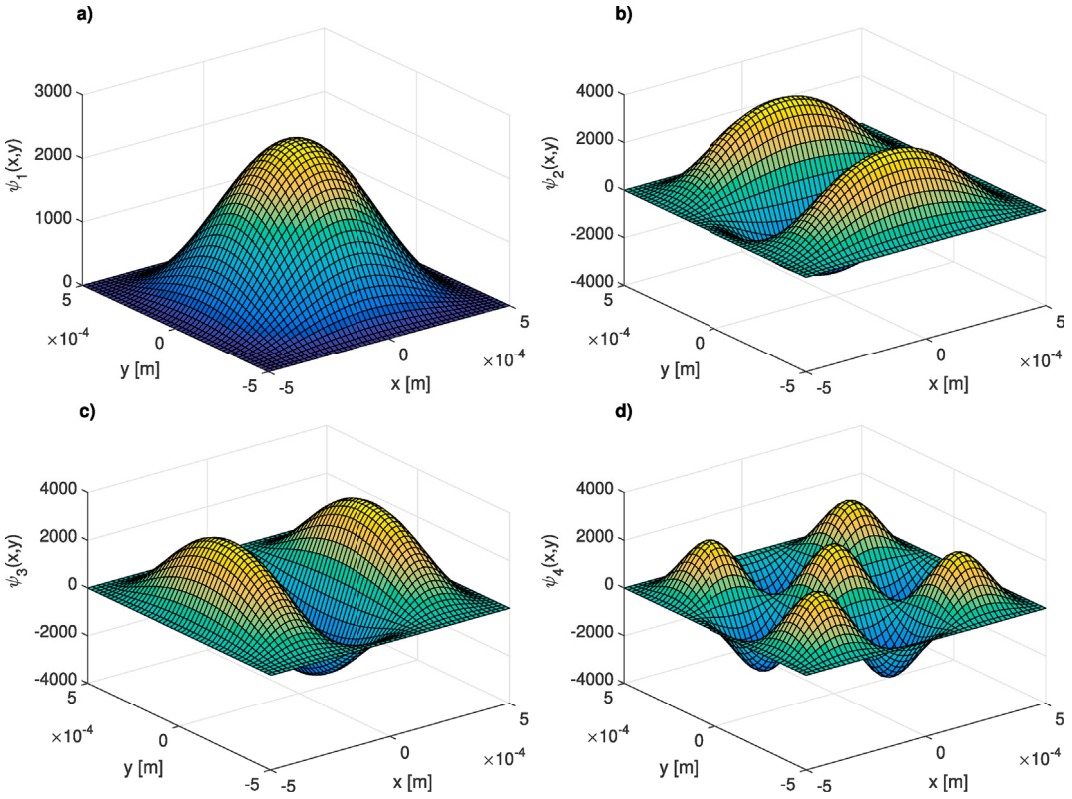

Fig. A.1 First four eigenfunctions $\psi_i(x,y), i = 1,2,3,4$, calculated using the method presented in this Appendix with $m,n = 1,2$: a) $\psi_1(x,y)$, b) $\psi_2(x,y)$, c) $\psi_3(x,y)$, d) $\psi_4(x,y)$.

The first four eigenfunctions $\psi_i(x,y), i = 1,2,3,4$, of the square clamped plate with the properties given in Table 2 obtained from the above described procedure in using the first four terms in the series (A.5) (the dimension of the matrices in equation (A.3a) is 4×4) are depicted in Fig. A.1. As an example the mean error of the first mode $\psi_1(x,y)$ (comparing to the reference numerical result ψ_{1num} computed using the Comsol Multiphysics software) has been calculated as follows

$$Err = \sqrt{\frac{\sum_{j=1}^{M} [\psi_{1num}(x_j,y_j) - \psi_1(x_j,y_j)]^2}{\sum_{j=1}^{M} \psi_{1num}^2(x_j,y_j)}} \cdot 100\%, \tag{A.6}$$

where ψ_{1num} is the reference eigenfunction calculated numerically using a mesh with $M = 50,225$ nodes, x_j, y_j being the coordinates of the j-th node of the mesh. In using the first four terms in the series (A.5) ($m,n = 1,2$) this error is 0.35% and decreases with the increasing number of terms considered in the series.

The eigenfrequencies calculated from the eigenvalues k_i using the relation

$$f_i = \frac{k_i^2}{2\pi}\sqrt{\frac{D}{M_s}} \tag{A.7}$$

are compared with the eigenfrequencies given by the numerical solution using Comsol Multiphysics and with the eigenfrequencies calculated from the values of $\omega(2a)^2\sqrt{M_s/D}$ given by Leissa [15], p. 61, 62, in the four Tables 4.24–4.27 (providing an interval of values). This comparison is summarized in Table A.1 for the first four modes and shows that the discrepancies between the results of the present method (using the first four terms of the series (A.5), $m,n = 1,2$), the reference numerical results, and the results taken from the literature remain very small. Table A.2 then presents the dependence of the values of the first four eigenfrequencies calculated using the present method on the number of the terms in the series (A.5).

Table A.1
Comparison of the values of eigenfrequencies given by the present method (for $m, n = 1, 2$), Comsol Multiphysics, and Leissa [15] (interval of values from the four Tables 4.24–4.27).

	Eigenfrequencies f_i [kHz]		
Mode i	Present method ($m, n = 1, 2$)	Comsol Multiphysics	Leissa [15] Tables 4.24–4.27 (interval)
1	142.405	142.140	138.819–142.530
2	521.130	518.490	520.591–523.557
3	523.352	520.990	520.591–525.613
4	875.800	865.120	867.401–887.887

Table A.2
Eigenfrequencies given by the present method for different number of values of m, n.

	Eigenfrequencies f_i [kHz]			
Mode i	$m, n = 1$	$m, n = 1, 2$	$m, n = 1, 2, 3$	$m, n = 1, 2, 3, 4$
1	142.808	142.405	142.345	142.329
2	–	521.130	520.616	520.478
3	–	523.352	523.023	522.930
4	–	875.800	872.074	870.976

References

[1] G.M. Sessler, Silicon microphones, J. Audio Eng. Soc. 44 (1/2) (1996) 16–22.
[2] J. Estèves, L. Rufer, D. Ekeom, S. Basrour, Lumped-parameters equivalent circuit for condenser microphones modeling, J. Acoust. Soc. Am. 142 (2017) 2121–2132.
[3] M. Bruneau, A.-M. Bruneau, Z. Škvor, P. Lotton, An equivalent network modelling the strong coupling between a vibrating membrane and a fluid film, Acta Acustica 2 (C5) (1994) 223–232.
[4] M. Bruneau, A.-M. Bruneau, P. Dupire, A model for rectangular miniaturized microphones, Acta Acustica 3 (3) (1995) 275–282.
[5] P. Honzík, M. Bruneau, Acoustic fields in thin fluid layers between vibrating walls and rigid boundaries: integral method, Acta Acustica United Acustica 101 (4) (2015) 859–862.
[6] A.H. Nayfeh, M.I. Younis, A new approach to the modelling and simulation of flexible microstructures under the effect of squeeze film damping, J. Micromech. Microeng. 14 (2) (2004) 170–181.
[7] R.B. Darling, C. Hivick, J. Xu, Compact analytical modeling of squeeze film damping with arbitrary venting conditions using a Green's function approach, Sens. Actuators, A Phys. 70 (1) (1998) 32–41.
[8] T. Verdot, E. Redon, K. Ege, J. Czarny, C. Guianvarc'h, J.-L. Guyader, Microphone with planar nano-gauge detection: fluid-structure coupling including thermo-viscous effects, Acta Acustica United Acustica 102 (3) (2016) 517–529.
[9] H. Lhermet, T. Verdot, A. Berthelot, B. Desloges, F. Souchon, First microphones based on an in-plane deflecting micro-diaphragm and piezoresistive nano–gauges, in: Proceeding of the MEMS 2018 Congress, Belfast, Northern Ireland, Jan. 2018, pp. 249–252.
[10] T. Veijola, H. Kuisma, J. Lahdenperä, T. Ryhänen, Equivalent-circuit model of squeezed gas field in a silicon accelerometer, Sens. Actuators, A Phys. 48 (3) (1995) 239–248.
[11] T. Veijola, A. Lehtovuori, Numerical and analytical modeling of trapped gas in micromechanical squeeze-film dampers, J. Sound Vib. 319 (1) (2009) 606–621.
[12] C. Mydlarz, J. Salamon, J.P. Bello, The implementation of low-cost urban acoustic monitoring devices, Appl. Acoust. 117 (2017) 207–218.
[13] C. Guianvarc'h, R.M. Gavioso, G. Benedetto, L. Pitre, M. Bruneau, Characterisation of condenser microphones under different environmental conditions for accurate speed of sound measurements with acoustic resonators, Rev. Sci. Instrum. 80 (7) (2009) 07 4901.
[14] W. Frommhold, H.V. Fuchs, S. Sheng, Acoustic performance of membrane absorbers, J. Sound Vib. 170 (5) (1994) 621–636, https://doi.org/10.1006/jsvi.1994.1091.
[15] A.W. Leissa, Vibration of Plates, Scientific and Technical Information Division, Natl. Aeronaut. Space Adm., 1969.
[16] J.-L. Guyader, Vibrations des Milieux Continus, Herms-Lavoisier Paris, 2002.
[17] Th. Le Van Suu, S. Durand, M. Bruneau, On the modelling of a clamped plate loaded by a squeeze fluid film: application to miniaturized sensors, Acta Acustica united Acustica 96 (5) (2010) 923–935.
[18] P. Honzík, C. Guianvarc'h, M. Bruneau, Modeling of capacitive MEMS microphone with square membrane or plate using integral method, Procedia Eng. 120 (2015) 418–421.
[19] K. Abramova, P. Honzík, N. Joly, S. Durand, M. Bruneau, Modelling of a MEMS transducer with a square plate loaded by a thin fluid layer, in: Euronoise 2018. Heraklion, Crete, 27.05.2018 - 31.05.2018, European Acoustics Association, Madrid, 2018, s. 337-340. ISSN 2226-5147.
[20] A. Novak, P. Honzík, M. Bruneau, Dynamic behaviour of a planar micro-beam loaded by a fluid-gap: analytical and numerical approach in a high frequency range, benchmark solutions, J. Sound Vib. (2017), https://doi.org/10.1016/j.jsv.2017.04.026.
[21] COMSOL Multiphysics, Acoustics Module User's Guide, 2018.
[22] COMSOL Multiphysics, Structural Mechanics Module User's Guide, 2018.